



Article

# Crystal Structural Determination of SrAlD<sub>5</sub> with Corner-Sharing AlD<sub>6</sub> Octahedron Chains by X-ray and Neutron Diffraction

Toyoto Sato <sup>1,\*</sup> , Shigeyuki Takagi <sup>1</sup>, Magnus H. Sørby <sup>2</sup> , Stefano Deledda <sup>2</sup>, Bjørn C. Hauback <sup>2</sup> and Shin-ichi Orimo <sup>1,3</sup>

<sup>1</sup> Institute for Materials Research, Tohoku University, 2-1-1 Katahira, Aoba-ku, Sendai 980-8577, Japan; shigeyuki.takagi@imr.tohoku.ac.jp (S.T.); orimo@imr.tohoku.ac.jp (S.O.)

<sup>2</sup> Institute for Energy Technology, P.O. Box 40, NO-2027 Kjeller, Norway; magnuss@ife.no (M.H.S.); stefano.deledda@ife.no (S.D.); bjorn.hauback@ife.no (B.C.H.)

<sup>3</sup> WPI-Advanced Institute for Materials Research, Tohoku University, 2-1-1 Katahira, Aoba-ku, Sendai 980-8577, Japan

\* Correspondence: toyoto@imr.tohoku.ac.jp; Tel.: +81-22-215-2094

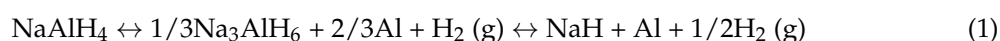
Received: 17 January 2018; Accepted: 7 February 2018; Published: 9 February 2018

**Abstract:** Aluminium-based complex hydrides (alanates) composed of metal cation(s) and complex anion(s), [AlH<sub>4</sub>]<sup>−</sup> or [AlH<sub>6</sub>]<sup>3−</sup> with covalent Al–H bonds, have attracted tremendous attention as hydrogen storage materials since the discovery of the reversible hydrogen desorption and absorption reactions on Ti-enhanced NaAlH<sub>4</sub>. In cases wherein alkaline-earth metals (M) are used as a metal cation, MAlH<sub>5</sub> with corner-sharing AlH<sub>6</sub> octahedron chains are known to form. The crystal structure of SrAlH<sub>5</sub> has remained unsolved although two different results have been theoretically and experimentally proposed. Focusing on the corner-sharing AlH<sub>6</sub> octahedron chains as a unique feature of the alkaline-earth metal, we here report the crystal structure of SrAlD<sub>5</sub> investigated by synchrotron radiation powder X-ray and neutron diffraction. SrAlD<sub>5</sub> was elucidated to adopt an orthorhombic unit cell with  $a = 4.6226(10)$  Å,  $b = 12.6213(30)$  Å and  $c = 5.0321(10)$  Å in the space group *Pbcm* (No. 57) and  $Z = 4$ . The Al–D distances (1.77–1.81 Å) in the corner-sharing AlD<sub>6</sub> octahedra matched with those in the isolated [AlD<sub>6</sub>]<sup>3−</sup> although the D–Al–D angles in the penta-alanates are significantly more distorted than the isolated [AlD<sub>6</sub>]<sup>3−</sup>.

**Keywords:** crystal structure; powder X-ray diffraction; powder neutron diffraction

## 1. Introduction

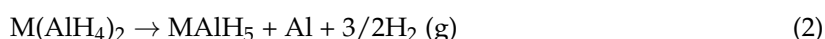
Aluminium-based complex hydrides (alanates) composed of metal cation(s) (typically alkali or alkaline-earth metals) and a complex anion, [AlH<sub>4</sub>]<sup>−</sup> or [AlH<sub>6</sub>]<sup>3−</sup> with covalent Al–H bonds, have attracted tremendous attention as hydrogen storage materials since Bogdanović and Schwickardi reported the reversible hydrogen desorption and absorption reactions on Ti-enhanced NaAlH<sub>4</sub> (Equation (1)) [1–5].



NaAlH<sub>4</sub> is composed of Na<sup>+</sup> and [AlH<sub>4</sub>]<sup>−</sup>, and Na<sub>3</sub>AlH<sub>6</sub> is composed of Na<sup>+</sup> and [AlH<sub>6</sub>]<sup>3−</sup>; hereafter, these as referred to as Na tetra-alanates and Na hexa-alanates, respectively.

In addition to studies on NaAlH<sub>4</sub> with Ti-based additives as hydrogen storage materials, exploratory studies on new alanates with different metal cations have also been conducted. Interestingly, alkaline-earth metal tetra-alanates M(AlH<sub>4</sub>)<sub>2</sub> composed of an alkaline-earth metal (M) and [AlH<sub>4</sub>]<sup>−</sup> decompose into MAlH<sub>5</sub> containing corner-sharing AlH<sub>6</sub> octahedron chains [3,6–9]

after releasing hydrogen from  $M(\text{AlH}_4)_2$  (Equation (2)). We refer to  $\text{MAlH}_5$  as an alkaline-earth metal penta-alanate.



Alanates with alkali metals, such as  $\text{NaAlH}_4$  [1–5], or mixed alkali and alkaline-earth metal cations, such as  $\text{LiCa}(\text{AlH}_4)_3$  [10], do not form alanates with corner-sharing  $\text{AlH}_6$  octahedron chains. Therefore, the corner-sharing  $\text{AlH}_6$  octahedron chains are a unique feature of alanates composed of alkaline-earth metals. Although the crystal structures of  $\text{CaAlH}_5$  [6–8] and  $\text{BaAlH}_5$  [9] have been experimentally and theoretically identified, the structures of  $\text{BeAlH}_5$ ,  $\text{MgAlH}_5$  and  $\text{SrAlH}_5$  have so far not been experimentally proven.  $\text{BeAlH}_5$  and  $\text{MgAlH}_5$  may be difficult to form due to the small size of  $\text{Be}^{2+}$  and  $\text{Mg}^{2+}$ . By contrast,  $\text{SrAlH}_5$  could be formed based on the size of the  $\text{Sr}^{2+}$ . Indeed, two crystal structures for  $\text{SrAlH}_5$  have been theoretically and experimentally proposed by Klaveness et al. [7] and Pommerin et al. [11], respectively. Both crystal structures have similar orthorhombic unit cells with  $a \approx 4.6 \text{ \AA}$ ,  $b \approx 5.0 \text{ \AA}$  and  $c \approx 12.7 \text{ \AA}$ , but different space groups. The theoretically proposed crystal structure was adopted the space group  $P2_12_12_1$  (No. 19) with a  $\text{BaAlF}_5$ -type crystal structure. The experimentally proposed crystal structure was described in space group  $Pnma$  (No. 62). Since the crystal structure reported by Pommerin et al. was studied using conventional powder X-ray diffraction, the positions of the hydrogen atom have not been determined. Even though  $P2_12_12_1$  is a subgroup of  $Pnma$ , the two proposed crystal structures give markedly different simulated powder X-ray diffraction patterns [11]. This demonstrates that they do not only differ with respect to inclusion of hydrogen but also have significantly different Sr–Al sublattice. Thus, the crystal structure of  $\text{SrAlH}_5$  remains unclarified. In the context of exploratory studies on new alanates, various Sr–Al hydrides with covalent Al–H bonds, including  $\text{SrAlSiH}$  [12],  $\text{SrAl}_2\text{H}_2$  [12,13],  $\text{Sr}(\text{AlH}_4)\text{Cl}$  [10] and  $\text{Sr}_2\text{AlH}_7$  [14], have been reported. In the alanate family, Sr forms the most diverse set of Al-based (complex) hydrides with covalent Al–H bonds. For further understanding of alanates, a complete crystal structure determination of  $\text{SrAlH}_5$  would be indispensable.

Therefore, we here report the crystal structure of  $\text{SrAlH}_5$  using synchrotron radiation powder X-ray (SR-PXD) and powder neutron diffraction (PND) on isotopically labelled  $\text{SrAlD}_5$ . Furthermore, we discuss the crystal structures of  $\text{MAlH}_5$ , related alanates and Al-based hydrides with covalent Al–H distances viewed from dependences of metal cations.

## 2. Materials and Methods

$\text{SrAlD}_5$  was synthesised by heat-treatment of mechanochemical milled  $\text{SrD}_2$  and  $\text{AlD}_3$  in the molar ratio 1:2 at 428 K for 1 h in Ar atmosphere of 0.1 MPa.  $\text{SrD}_2$  as the starting material was synthesised from dendritic pieces of Sr (Sigma-Aldrich, St. Louis, MO, USA, 99.99%) at 673 K for 10 h in a deuterium gas pressure of 0.5 MPa.  $\text{AlD}_3$  as the starting material was synthesised in diethyl ether according to the chemical reaction of  $\text{LiAlD}_4$  and  $\text{AlCl}_3$  [15,16]. The mixture of  $\text{SrD}_2$  and  $\text{AlD}_3$  was ball-milled at 400 r.p.m. under a deuterium gas pressure of 0.3 MPa using a Fritsch P7. The effective milling time was 3 h. Milling times of 15 min were alternated with pauses of 5 min duration, similar to our previous study [8,10,17].

$\text{SrAlD}_5$  was initially measured using a conventional powder X-ray diffractometer (PXD, PANalytical X'PERT, Almelo, Netherlands, with Cu  $K\alpha$  radiation (wavelength  $\lambda = 1.5406 \text{ \AA}$  for  $K\alpha_1$  and  $1.5444 \text{ \AA}$  for  $K\alpha_2$ ) at room temperature. The sample for PXD was placed in a Lindemann glass capillary (outside diameter = 0.50 mm, thickness = 0.01 mm) and sealed with paraffin liquid for the PXD measurement with a transmission geometry at room temperature.

The high-resolution SR-PXD data of  $\text{SrAlD}_5$  were collected at room temperature at the Swiss-Norwegian beamlines (station BM01B) at the European Synchrotron Radiation Facility (ESRF) in Grenoble, France. The sample was placed in a rotating 0.5 mm borosilicate glass capillary. The wavelength of  $0.5053 \text{ \AA}$  was obtained from a channel-cut Si (111) monochromator. Data were collected up to  $40^\circ$  in steps of  $0.0065^\circ$  in  $2\theta$  with 6 scintillator detectors fitted with analyser crystals.

The PND data of SrAlD<sub>5</sub> were collected at 10 K and room temperature using the PUS instrument at the JEEP II reactor in Kjeller, Norway. The sample was placed in a cylindrical vanadium sample holder with a diameter of 6 mm. The wavelength of 1.5539 Å was obtained from a Ge (511) focusing monochromator. Data were collected from 10° to 130° and binned in steps of 0.05° in 2θ.

The PXD peaks of SrAlD<sub>5</sub> were indexed by TREOR97 [18] to determine the initial unit cell parameters for the structural determinations. Crystal structure determinations of SrAlD<sub>5</sub> with SR-PXD and PND data were performed combined with the ab initio structural determination programme FOX (version 1.9.0.2) [19] and the Rietveld programme GSAS with the graphical interface EXPGUI (version 1.80) [20]. FOX is used for determination of an initial crystal structure model and GSAS is used for the refinements of the initial crystal structure model. In the Rietveld analysis, the Pseudo-Voigt peak shape function with the Finger-Cox-Jephcoat asymmetry correction [21,22] was used. The background for SR-PXD and PND was modelled using the Chebyshev polynomial function in GSAS with 12 terms. Al–D distances in SrAlD<sub>5</sub> were refined using a soft restraint, Al–D = 1.80 Å and Sr–D = 2.45 Å. Al and SrD<sub>2</sub> were added as the impurity phases for the Rietveld refinement.

All samples were handled in Ar filled glove boxes with a dew point below 183 K and with less than 1 ppm of O<sub>2</sub> to prevent (hydro-) oxidation.

### 3. Results

The synthesised sample, which was obtained from heat-treatment of mechanochemical milled SrD<sub>2</sub> and AlD<sub>3</sub> in the molar ratio of 1:2 at 428 K for 1 h in Ar atmosphere of 0.1 MPa, was characterised using conventional powder X-ray diffraction (Figure S1 in the Supplementary Material). Bragg peaks from metallic Al and unreacted SrD<sub>2</sub> were easily identified. Al originated from AlD<sub>3</sub> decomposition or the mechanochemical milled SrD<sub>2</sub> + 2AlD<sub>3</sub> since the presence of a complex anion, [AlD<sub>4</sub>]<sup>−</sup>, in the mechanochemical milled sample was identified by Raman spectroscopy. This confirms that Sr(AlD<sub>4</sub>)<sub>2</sub> could be obtained from mechanochemical milling of SrD<sub>2</sub> + 2AlD<sub>3</sub> as reported in previous works [8,10,17] although the crystal structure of Sr(AlD<sub>4</sub>)<sub>2</sub> could not be determined due to its poor crystallinity. The remaining Bragg peaks were indexed by an orthorhombic unit cell with  $a \approx 4.66$  Å,  $b \approx 12.71$  Å and  $c \approx 5.03$  Å, and these values are close to the theoretically and experimentally reported unit cell parameters of SrAlH<sub>5</sub> [7,11]. Therefore, SrAlD<sub>5</sub> is the main phase present in the synthesised sample (the differences between this study and the past studies will be addressed in detail in the discussion).

Considering the reflection conditions on the obtained orthorhombic unit cell, possible space groups were selected. Then, the ab initio structural determination programme FOX (version 1.9.0.2) [19] was performed on the orthorhombic unit cell with the selected space group and the SR-PXD and PND measured at room temperature for finding an initial crystal structure model for Rietveld refinement. All possible initial crystal structure models were attempted to be refined by the Rietveld programme GSAS with the graphical interface EXPGUI (version 1.80) [20]. Finally, the measured SR-PXD and PND patterns at room temperature are reasonably reproduced by SrAlD<sub>5</sub> with  $a = 4.6226(10)$  Å,  $b = 12.6213(30)$  Å and  $c = 5.0321(10)$  Å in the space group *Pbcm* (No. 57) and  $Z = 4$  (Figure 1a). The crystal structure is illustrated in Figure 1b. The crystallographic parameters are listed in Table 1. SrAlD<sub>5</sub> was clarified to adopt corner-sharing AlD<sub>6</sub> octahedron chains as the other penta-alanates. The inter-atomic distances of Al–D (1.77–1.81 Å) and Sr–D (2.46–3.04 Å) are listed in Table 2, which clearly shows that the both inter-atomic distances were reasonable compared with binary hydrides AlD<sub>3</sub> [3] and SrD<sub>2</sub> [23] or alanates and aluminium-based complex hydrides with AlD<sub>6</sub> units [3] (discussed later).

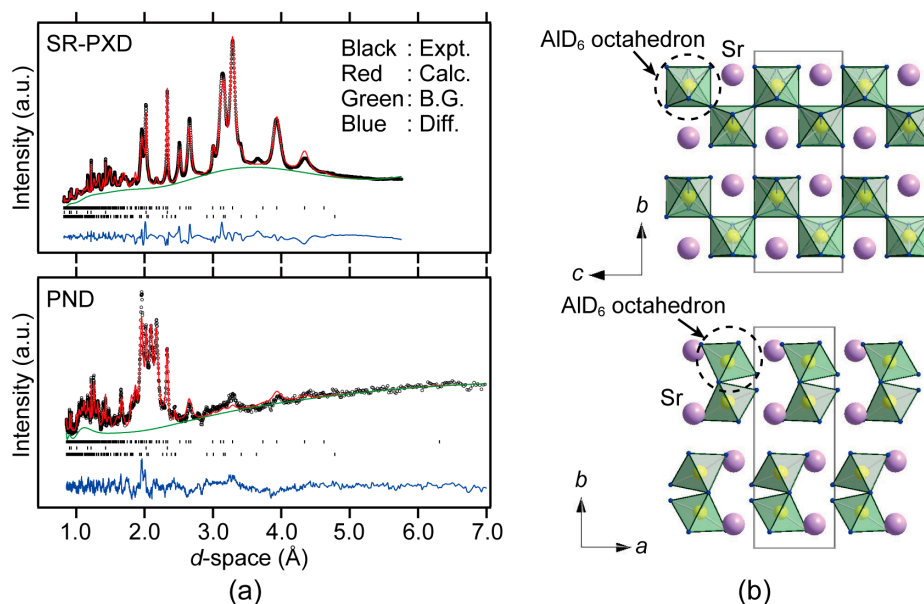


**Figure 1.** (a) The Rietveld refinement fits of (upper) SR-PXD ( $R_{wp} = 0.0306$ ) with  $\lambda = 0.5053$  Å and (lower) PND ( $R_{wp} = 0.0429$ ) with  $\lambda = 1.5539$  Å for SrAlD<sub>5</sub> and (b) the crystal structure of SrAlD<sub>5</sub> viewed along the a-axis (upper) and c-axis (lower). Purple, yellow and blue spheres and light-green octahedra represent Sr, Al, D and AlD<sub>6</sub>, respectively. In the Rietveld refinement fits of SR-PXD and PND, the observed, calculated background and difference between observed and calculated patterns are indicated with circles, a red, green and blue lines, respectively. The Bragg reflection positions are shown for (top) SrAlD<sub>5</sub>, (middle) Al and (bottom) SrD<sub>2</sub>. The refined weight fractions of SrAlD<sub>5</sub>, Al and SrD<sub>2</sub> were 75 wt % (84 wt %), 20 wt % (13 wt %) and 5 wt % (3 wt %), respectively (PND are provided in parentheses).

**Table 1.** Crystallographic parameters for SrAlD<sub>5</sub> with  $a = 4.6226(10)$  Å,  $b = 12.6213(30)$  Å and  $c = 5.0321(10)$  Å obtained from both of SR-PXD and PND in the space group  $Pbcm$  (No. 57) and  $Z = 4$ . The  $U_{iso}$  of Al was not refined and the occupancies of each atomic position were fixed as 1.00. Estimated standard deviations are in parentheses.

Atom	Wyckoff Position	$x$	$y$	$z$	$100 \times U_{iso}$ (Å <sup>2</sup> )
Sr	4d	0.2532(7)	0.8925(3)	0.2500	0.13(3)
Al	4d	0.3296(11)	0.1597(3)	0.2500	1.00
D1	4c	0.4366(13)	0.2500	0.0000	4.75(15)
D2	4d	0.3461(13)	0.5790(5)	0.2500	4.75(15)
D3	4d	0.0311(13)	0.7146(3)	0.2500	4.75(15)
D4	8e	0.1914(7)	0.0718(3)	0.4986(9)	4.75(15)

**Table 2.** Inter-atomic distances of SrAlD<sub>5</sub>. Estimated standard deviations are in parentheses.

Inter-Atomic Distances (Å)	
Sr–D1	$2.621(4) \times 2$
Sr–D2	$2.5776(19) \times 2$ $2.996(7)$
Sr–D3	$2.4686(24)$ $3.035(4) \times 2$
Sr–D4	$2.4549(17) \times 2$ $2.602(4) \times 2$ $2.898(5) \times 2$
Al–D1	$1.7683(30) \times 2$
Al–D2	$1.812(5)$
Al–D3	$1.806(4)$
Al–D4	$1.7901(29) \times 2$

#### 4. Discussion

The different proposed crystal structure models and their simulated diffraction patterns are shown in Figure S2 in the Supplementary Material. All crystal structure models show orthorhombic unit cells but in different space groups. The crystal structure reported by Pommerin et al. shows a similar SR-PXD pattern as the one calculated using our crystal structure model despite the lack of hydrogen or deuterium atoms. This shows that the both metal atomic arrangements are nearly identical to our crystal structure model. By contrast, the crystal structure reported by Klaveness et al. neither fits with the SR-PXD nor PND from our crystal structure model. Attempts to refine the *Pnma* model from Pommerin et al. with our data, resulted in highly distorted  $\text{AlD}_6$  octahedra and poor fits to both SR-PXD and PND. The model and fits did not improve significantly by reducing the symmetry from *Pnma* (No. 62) to space group  $P2_12_12_1$  (No. 19) which is a subgroup of *Pnma* (No. 62). The PND pattern remained largely unchanged at 10 K (not shown). This indicates that  $\text{SrAlD}_5$  does not undergo any crystal structure transitions at lower temperatures. Therefore,  $\text{SrAlD}_5$  cannot be accurately represented by the space group *Pnma* (No. 62) nor the space group  $P2_12_12_1$  (No. 19), neither at room temperatures nor 10 K. The new model presented here is the most reasonable crystal structure for  $\text{SrAlD}_5$ .

The crystal structure data for  $\text{MAID}_5$  compounds (M: Ca, Sr, Ba) and the average Al–D, M–D and M–Al distances are listed in Table 3 [8,9]. The  $\text{AlD}_6$  octahedron chains in  $\text{MAID}_5$  are illustrated in Figure 2. The average Al–D distances in  $\text{MAID}_5$  are unaffected by the cation size. They are in the range of 1.75–1.80 Å whereas the average M–D or M–Al distances increase with increasing metal cation radius. Focusing on the  $\text{AlD}_6$  octahedron chains in  $\text{MAID}_5$ , the  $\text{AlD}_6$  octahedron, viewed along the  $\text{AlD}_6$  octahedron chains, appears qualitatively more canted as the metal cation radius decreases (Figure 2). Indeed, the ionic radius of  $\text{Ca}^{2+}$  is markedly smaller than  $\text{Sr}^{2+}$  and  $\text{Ba}^{2+}$  and  $\text{CaAlD}_5$  takes a more complex monoclinic structure with twice the number of formula units per unit cell compared to the orthorhombic  $\text{SrAlD}_5$  and  $\text{BaAlD}_5$ . This suggests that  $\text{BeAlH}_5$  and  $\text{MgAlH}_5$  might be speculated to have low symmetry structures with large unit cells if  $\text{BeAlH}_5$  and  $\text{MgAlH}_5$  could be formed.

In the context of  $\text{SrAlH}_5$ , Pommerin et al. also reported that  $\text{EuAlH}_5$  exhibited an isomorphic crystal structure similar to  $\text{SrAlH}_5$  in spite of the rare-earth metal [11]. This might originate into size and valence of cation metals because  $\text{Eu}^{2+}$  has close ionic radius to  $\text{Sr}^{2+}$  [24] and trivalent rare-earth metals do not yield the  $\text{AlH}_6$  octahedron chains but isolated  $\text{AlH}_6$  ( $[\text{AlH}_6]^{3-}$ ) [25]. Although only  $\text{EuAlH}_5$  has been experimentally identified, divalent rare-earth metals with close ionic radius to  $\text{Ca}^{2+}$ ,  $\text{Sr}^{2+}$  and  $\text{Ba}^{2+}$  would be speculated to form penta-alanates such as  $\text{EuAlH}_5$ .

**Table 3.** Crystal structure data for  $\text{MAID}_5$  and selected inter-atomic distances and angles (Estimated standard deviations for  $\text{SrAlD}_5$  are in parentheses).

	Crystal System (Space Group)	Unit Cell Parameters	Z	Avg. Al–D Distances	D–Al–D Angles	Avg. M–D Distances	Avg. M–Al Distances
$\text{CaAlD}_5$ [8]	Monoclinic ( $P2_1/c$ )	$a = 9.800 \text{ \AA}$ $b = 6.908 \text{ \AA}$ $c = 12.450 \text{ \AA}$ $\beta = 137.94^\circ$ $V = 564.69 \text{ \AA}^3$	8	1.75 Å	$78.0^\circ\text{--}101.8^\circ$ $166.6^\circ\text{--}177.9^\circ$	2.43 Å	3.50 Å
$\text{SrAlD}_5$ (present result)	Orthorhombic ( $Pbcm$ )	$a = 4.6226(10) \text{ \AA}$ $b = 12.6213(30) \text{ \AA}$ $c = 5.0321(10) \text{ \AA}$ $V = 293.59(12) \text{ \AA}^3$	4	1.79(2) Å	$84.7(2)^\circ\text{--}97.5(3)^\circ$ $168.4(3)^\circ\text{--}175.3(3)^\circ$	2.70(21) Å	3.55(26) Å
$\text{BaAlD}_5$ [9]	Orthorhombic ( $Pna2_1$ )	$a = 9.194 \text{ \AA}$ $b = 7.040 \text{ \AA}$ $c = 5.106 \text{ \AA}$ $V = 330.51 \text{ \AA}^3$	4	1.77 Å	$75.7^\circ\text{--}103.7^\circ$ $161.4^\circ\text{--}169.9^\circ$	2.82 Å	3.68 Å

Figure 3 shows the metal cation dependences on the average metal cation–Al and Al–D distances [3,8–10,12–14,25–37] in related alanates (deuterides) with covalent Al–D bonds. The average Al–D distances in corner-sharing  $\text{AlD}_6$  octahedra in  $\text{MAID}_5$  are consistent with those found in



hexa-alanates [3],  $\text{Sr}_2\text{AlD}_7$  [14] and  $\text{Ba}_2\text{AlD}_7$  [26]. However the D–Al–D angles in the penta-alanates (Table 3) are significantly more distorted than those in the compounds with isolated  $\text{AlD}_6$  octahedron. Thus the corner-sharing in the penta-alanates slightly affect the D–Al–D angles of the octahedron. Besides, the average Al–D distances were not affected by the metal cations (Al–D  $\approx$  1.60 Å ( $[\text{AlD}_4]^-$ ), 1.80 Å ( $[\text{AlD}_6]^{3-}$  and  $\text{AlD}_6$  octahedron) and 1.75 Å ( $\text{SrAlSiD}$  and  $\text{SrAl}_2\text{D}_2$ )). By contrast, the average metal cation–Al distance was elongated with increasing metal cation radius. Interestingly, the average metal cation–Al distance in the penta-alanates and hexa-alanates was shorter than that with  $[\text{AlD}_4]^-$  in tetra-alanates, even though  $[\text{AlD}_6]^{3-}$  ( $\text{AlH}_6$  octahedron) has a bigger radius than  $[\text{AlD}_4]^-$  ( $[\text{AlD}_4]^-$ : 2.26 Å;  $[\text{AlD}_6]^{3-}$ : 2.56 Å [38]). Focusing on the ionic filling fractions (IFF) [10], as defined by the volumes of the crystal structure and the constituent ions in their ionic compounds including alanates, the average IFF for tetra-alanates and hexa-alanates are 0.72 and 0.79, respectively, indicating that hexa-alanates have tighter ionic (atomic) packing than tetra-alanates. This would explain the shorter average metal cation–Al distance with the  $[\text{AlD}_6]^{3-}$  ( $\text{AlD}_6$  octahedron) compared to that with  $[\text{AlD}_4]^-$ .

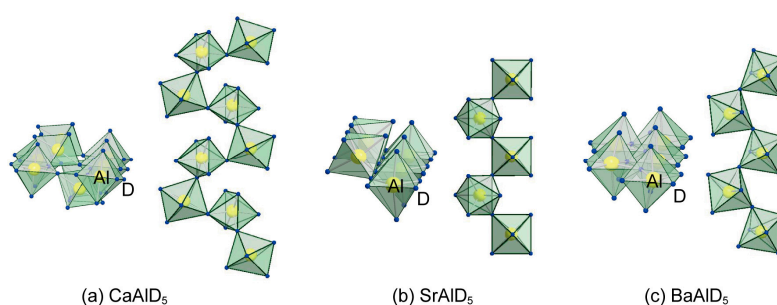


**Figure 2.** Corner-sharing  $\text{AlD}_6$  octahedron chains viewed from (left) along and (right) perpendicular to the chains in (a)  $\text{CaAlD}_5$ , (b)  $\text{SrAlD}_5$  and (c)  $\text{BaAlD}_5$  (Al: yellow sphere; D: blue sphere).

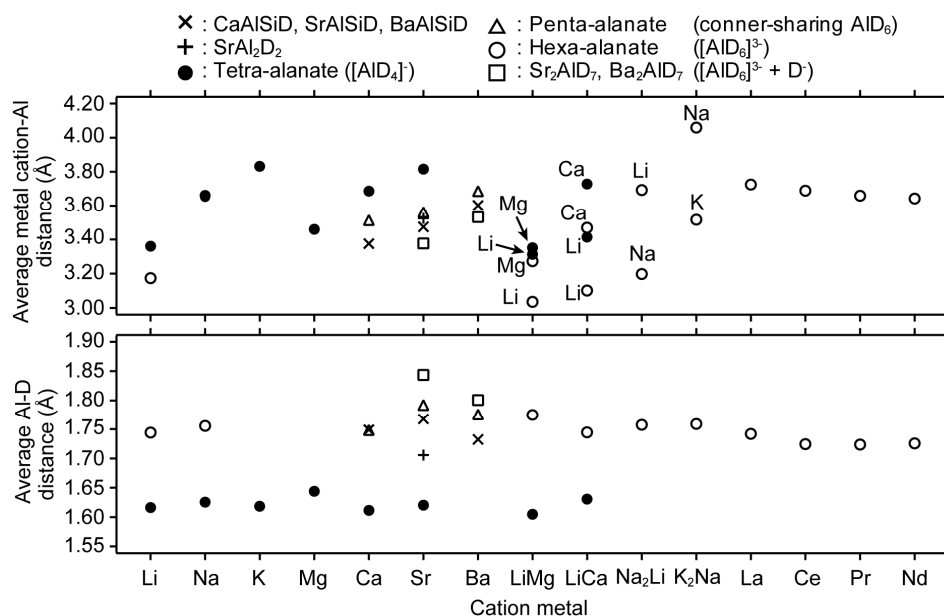


**Figure 3.** Metal cation dependences on (upper) average metal cation–Al and (lower) Al–D distances in alanates and related Al-based hydrides. The distances were obtained from their deuterides, except for  $\text{Mg}(\text{AlH}_4)_2$ ,  $\text{LiCa}(\text{AlH}_4)_3$ ,  $\text{LiCaAlH}_6$ ,  $\text{K}_2\text{NaAlH}_6$ ,  $\text{LaAlH}_6$ ,  $\text{CeAlH}_6$ ,  $\text{PrAlH}_6$  and  $\text{NdAlH}_6$  ( $\text{LiCa}(\text{AlH}_4)_3$  and  $\text{LiCaAlH}_6$  are theoretical calculation results [3,8–10,12–14,25–37] because their crystal structural investigations on deuterides have not been reported. Average metal cation–Al distance of  $\text{Na}_3\text{AlD}_6$  (3.65 Å) [33] is overlapped with  $\text{NaAlD}_4$  (3.66 Å) [28]. In  $\text{CaAlSiD}$ ,  $\text{SrAlSiD}$ ,  $\text{BaAlSiD}$  and  $\text{SrAl}_2\text{D}_2$ , Ca, Sr and Ba were formally considered as their metal cation.

## 5. Conclusions

Focusing on the corner-sharing  $\text{AlH}_6$  octahedron chains as a unique feature of the alkaline-earth metal, we determined the crystal structure of  $\text{SrAlD}_5$ , which adopted an orthorhombic unit cell with  $a = 4.6226(10)$  Å,  $b = 12.6213(30)$  Å and  $c = 5.0321(10)$  Å in the space group  $Pbcm$  (No. 57) and  $Z = 4$ , using synchrotron radiation powder X-ray and neutron diffraction. The crystal structure comprised corner-sharing  $\text{AlD}_6$  octahedron chains with  $\text{Al-D} = 1.76\text{--}1.81$  Å.

Compared with the corner-sharing  $\text{AlD}_6$  octahedron chains in  $\text{CaAlD}_5$ ,  $\text{SrAlD}_5$  and  $\text{BaAlD}_5$  (penta-alanates), the structure and tilt of the  $\text{AlD}_6$  was observed to become more complex as the cation becomes smaller. If  $\text{BeAlD}_5$  and  $\text{MgAlD}_5$ , which have not been experimentally identified, could be formed, they might have low symmetry structures with large unit cells.

Furthermore, the crystal structures of penta-alanates with corner-sharing  $\text{AlD}_6$  octahedron chains were compared with Al-based complex hydrides composed of metal cation(s) and complex anion(s),  $[\text{AlD}_4]^-$  and  $[\text{AlD}_6]^{3-}$ , as well as with Al-based hydrides with covalent Al-D bonds. The geometry of  $\text{AlD}_6$  octahedra in corner-sharing chains was found to be similar to isolated  $[\text{AlD}_6]^{3-}$  complex anions although the D-Al-D angles are distorted. In addition, the metal cation-Al distances shortened as the complex anion radius became larger (radius of  $[\text{AlD}_6]^{3-} >$  radius of  $[\text{AlD}_4]^-$ ) although the Al-D distances were unaffected by the metal cations. This originates from the ionic filling fractions, according to which the hexa-alanates composed of metal cations and the  $[\text{AlD}_6]^{3-}$  complex anion have tighter ionic (atomic) packing crystal structures than the tetra-alanates composed of metal cations and the  $[\text{AlD}_4]^-$  complex anion.

**Supplementary Materials:** The following are available online at [www.mdpi.com/2073-4352/8/2/89/s1](http://www.mdpi.com/2073-4352/8/2/89/s1), Figure S1: Conventional powder X-ray diffraction pattern of  $\text{SrAlD}_5$ ; Figure S2: (a) Simulated SR-PXD and PND patterns and (b) crystal structures of  $\text{SrAlD}_5$  on the present work and reported by Klaveness et al. and Pommerin et al.

**Acknowledgments:** We are grateful for the technical support from H. Ohmiya and N. Warifune. This research was supported by the JSPS KAKENHI Grant Numbers 16K06766, 16H06119 and 25220911 from MEXT, Japan, and Collaborative Research Center on Energy Materials in IMR (E-IMR), Institute for Materials Research, Tohoku University. The skillful assistance of the beamline personnel at the Swiss-Norwegian Beamlines at the European Synchrotron Radiation Facility (ESRF), Grenoble, France, is gratefully acknowledged.

**Author Contributions:** T.S. conceived this study, prepared and characterized the samples, analyzed the SR-PXD and the PND data, determined the crystal structure and wrote the manuscript; S.T. determined the crystal structure; M.H.S., S.D. and B.C.H. performed the SR-PXD and the PND; S.O. designed and conducted the project.

**Conflicts of Interest:** The authors declare no conflict of interest.

## References

1. Bogdanović, B.; Schwickardi, M. Ti-doped alkali metal aluminium hydrides as potential novel reversible hydrogen storage materials. *J. Alloy. Compd.* **1997**, *253–254*, 1–9. [[CrossRef](#)]
2. Orimo, S.; Nakamori, Y.; Eliseo, R.J.; Züttel, A.; Jensen, C.M. Complex hydrides for hydrogen storage. *Chem. Rev.* **2007**, *107*, 4111–4132. [[CrossRef](#)] [[PubMed](#)]
3. Hauback, B. Structures of aluminium-based light weight hydrides. *Z. Krist.* **2008**, *223*, 636–648. [[CrossRef](#)]
4. Eberle, U.; Felderhoff, M.; Schüth, F. Chemical and physical solutions for hydrogen storage. *Angew. Chem. Int. Ed.* **2009**, *48*, 6608–6630. [[CrossRef](#)] [[PubMed](#)]
5. Graetz, J.; Hauback, B.C. Recent developments in aluminum-based hydrides for hydrogen storage. *MRS Bull.* **2013**, *38*, 473–479. [[CrossRef](#)]
6. Weidenthaler, C.; Frankcombe, T.J.; Felderhoff, M. First crystal structure studies of  $\text{CaAlH}_5$ . *Inorg. Chem.* **2006**, *45*, 3849–3851. [[CrossRef](#)] [[PubMed](#)]
7. Klaveness, A.; Vajeeston, P.; Ravindran, P.; Fjellvåg, H.; Kjekshus, A. Structure and bonding in  $\text{BAlH}_5$  ( $B = \text{Be, Ca, Sr}$ ) from first-principle calculations. *J. Alloy. Compd.* **2007**, *433*, 225–232. [[CrossRef](#)]
8. Sato, T.; Sørby, M.H.; Ikeda, K.; Sato, S.; Hauback, B.C.; Orimo, S. Syntheses, crystal structures, and thermal analyses of solvent-free  $\text{Ca}(\text{AlD}_4)_2$  and  $\text{CaAlD}_5$ . *J. Alloy. Compd.* **2009**, *487*, 472–478. [[CrossRef](#)]

9. Zhang, Q.-A.; Nakamura, Y.; Oikawa, K.; Kamiyama, T.; Akiba, E. New alkaline earth aluminum hydride with one-dimensional zigzag chains of  $[\text{AlH}_6]$ : Synthesis and crystal structure of  $\text{BaAlH}_5$ . *Inorg. Chem.* **2002**, *41*, 6941–6943. [[CrossRef](#)] [[PubMed](#)]
10. Sato, T.; Takagi, S.; Deledda, S.; Hauback, B.C.; Orimo, S. Goldschmidt tolerance factor to arbitrary ionic compounds. *Sci. Rep.* **2016**, *6*, 23592. [[CrossRef](#)] [[PubMed](#)]
11. Pommerin, A.; Wosylus, A.; Felderhoff, M.; Schüth, F.; Weidenthaler, C. Synthesis, crystal structures, and hydrogen-storage properties of  $\text{Eu}(\text{AlH}_4)_2$  and  $\text{Sr}(\text{AlH}_4)_2$  and of their decomposition intermediates,  $\text{EuAlH}_5$  and  $\text{SrAlH}_5$ . *Inorg. Chem.* **2012**, *51*, 4143–4150. [[CrossRef](#)] [[PubMed](#)]
12. Björling, T.; Noréus, D.; Jansson, K.; Andersson, M.; Leonova, E.; Edén, M.; Hålenius, U.; Häussermann, U.  $\text{SrAlSiH}$ : A polyanionic semiconductor hydride. *Angew. Chem. Int. Ed.* **2005**, *44*, 7269–7273. [[CrossRef](#)] [[PubMed](#)]
13. Gingl, F.; Vogt, T.; Akiba, E. Trigonal  $\text{SrAl}_2\text{H}_2$ : The first Zintl phase hydride. *J. Alloy. Compd.* **2000**, *306*, 127–132. [[CrossRef](#)]
14. Zhang, Q.-A.; Nakamura, Y.; Oikawa, K.; Kamiyama, T.; Akiba, E. Synthesis and crystal structure of  $\text{Sr}_2\text{AlH}_7$ : A new structural type of alkaline earth aluminum hydride. *Inorg. Chem.* **2002**, *41*, 6547–6549. [[CrossRef](#)] [[PubMed](#)]
15. Brower, F.M.; Matzek, N.E.; Reigler, P.F.; Rinn, H.W.; Roberts, C.B.; Schmidt, D.L.; Snover, J.A.; Terada, K. Preparation and properties of aluminum hydride. *J. Am. Chem. Soc.* **1976**, *98*, 2450–2453. [[CrossRef](#)]
16. Ikeda, K.; Muto, S.; Tatsumi, K.; Menjo, M.; Kato, S.; Biemann, M.; Züttel, A.; Jensen, C.M.; Orimo, S. Dehydrogenating reaction of  $\text{AlH}_3$ : In situ microscopic observations combined with thermal and surface analysis. *Nanotechnology* **2009**, *20*, 204004. [[CrossRef](#)] [[PubMed](#)]
17. Sato, T.; Ikeda, K.; Li, H.-W.; Yukawa, H.; Morinaga, M.; Orimo, S. Direct dry syntheses and thermal analyses of a series of aluminum complex hydrides. *Mater. Trans.* **2009**, *50*, 182–186. [[CrossRef](#)]
18. Werner, P.-E.; Eriksson, L.; Westdahl, M. TREOR, a semi-exhaustive trial-and-error powder indexing program for all symmetries. *J. Appl. Crystallogr.* **1985**, *18*, 367–370. [[CrossRef](#)]
19. Favre-Nicolin, V.; Černý, R. FOX, 'Free objects for crystallography': A modular approach to ab initio structure determination from powder diffraction. *J. Appl. Crystallogr.* **2002**, *35*, 734–743. [[CrossRef](#)]
20. Toby, B.H. EXPGUI, a graphical user interface for GSAS. *J. Appl. Crystallogr.* **2001**, *34*, 210–213. [[CrossRef](#)]
21. Van Laar, B.; Yelon, W.B. The peak in neutron powder diffraction. *J. Appl. Crystallogr.* **1984**, *17*, 47–54. [[CrossRef](#)]
22. Thompson, P.; Cox, D.E.; Hastings, J.B. Rietveld refinement of Debye-Scherrer synchrotron X-ray data from  $\text{Al}_2\text{O}_3$ . *J. Appl. Crystallogr.* **1987**, *20*, 79–83. [[CrossRef](#)]
23. Brese, N.E.; O'Keeffe, M.; Von Dreele, R.B. Synthesis and crystal structure of  $\text{SrD}_2$  and  $\text{SrND}$  and bond valence parameters for hydrides. *J. Solid State Chem.* **1990**, *88*, 571–576. [[CrossRef](#)]
24. Shannon, R.D. Revised effective ionic radii and systematic studies of interatomic distances in halides and chalcogenides. *Acta Crystallogr. A* **1976**, *32*, 751–767. [[CrossRef](#)]
25. Weidenthaler, C.; Pommerin, A.; Felderhoff, M.; Sun, W.; Wolverton, C.; Bogdanović, B.; Schüth, F. Complex rare-earth aluminum hydrides: Mechanochemical preparation, crystal structure and potential for hydrogen storage. *J. Am. Chem. Soc.* **2009**, *131*, 16735–16743. [[CrossRef](#)] [[PubMed](#)]
26. Zhang, Q.A.; Nakamura, Y.; Oikawa, K.; Kamiyama, T.; Akiba, E. Hydrogen-induced phase decomposition of  $\text{Ba}_7\text{Al}_{13}$  and the crystal structure of  $\text{Ba}_2\text{AlH}_7$ . *J. Alloy. Compd.* **2003**, *361*, 180–186. [[CrossRef](#)]
27. Hauback, B.C.; Brinks, H.W.; Fjellvåg, H. Accurate structure of  $\text{LiAlD}_4$  studied by combined powder neutron and X-ray diffraction. *J. Alloy. Compd.* **2002**, *346*, 184–189. [[CrossRef](#)]
28. Hauback, B.C.; Brinks, H.W.; Jensen, C.M.; Murphy, K.; Maeland, A.J. Neutron diffraction structure determination of  $\text{NaAlD}_4$ . *J. Alloy. Compd.* **2003**, *358*, 142–145. [[CrossRef](#)]
29. Hauback, B.C.; Brinks, H.W.; Heyn, R.H.; Blom, R.; Fjellvåg, H. The crystal structure of  $\text{KAlD}_4$ . *J. Alloy. Compd.* **2005**, *394*, 35–38. [[CrossRef](#)]
30. Fossdal, A.; Brinks, H.W.; Fichtner, M.; Hauback, B.C. Determination of the crystal structure of  $\text{Mg}(\text{AlH}_4)_2$  by combined X-ray and neutron diffraction. *J. Alloy. Compd.* **2005**, *387*, 47–51. [[CrossRef](#)]
31. Grove, H.; Brinks, H.W.; Heyn, R.H.; Wu, F.-J.; Opalka, S.M.; Tang, X.; Laube, B.L.; Hauback, B.C. The structure of  $\text{LiMg}(\text{AlD}_4)_3$ . *J. Alloy. Compd.* **2008**, *455*, 249–254. [[CrossRef](#)]
32. Brinks, H.W.; Hauback, B.C. The structure of  $\text{Li}_3\text{AlD}_6$ . *J. Alloy. Compd.* **2003**, *354*, 143–147. [[CrossRef](#)]



33. Rönnebro, E.; Noréus, D.; Kadir, K.; Reiser, A.; Bogdanovic, B. Investigation of the perovskite related structures of  $\text{NaMgH}_3$ ,  $\text{NaMgF}_3$  and  $\text{Na}_3\text{AlH}_6$ . *J. Alloy. Compd.* **2000**, *299*, 101–106. [[CrossRef](#)]
34. Grove, H.; Brinks, H.W.; Løvvik, O.M.; Heyn, R.H.; Hauback, B.C. The structure of  $\text{LiMgAlD}_6$  from combined neutron and synchrotron X-ray powder diffraction. *J. Alloy. Compd.* **2008**, *460*, 64–68. [[CrossRef](#)]
35. Brinks, H.W.; Hauback, B.C.; Jensen, C.M.; Zidan, R. Synthesis and crystal structure of  $\text{Na}_2\text{LiAlD}_6$ . *J. Alloy. Compd.* **2005**, *392*, 27–30. [[CrossRef](#)]
36. Sørby, M.H.; Brinks, H.W.; Fossdal, A.; Thorshaug, K.; Hauback, B.C. The crystal structure and stability of  $\text{K}_2\text{NaAlH}_6$ . *J. Alloy. Compd.* **2006**, *415*, 284–287. [[CrossRef](#)]
37. Lee, M.H.; Börling, T.; Hauback, B.C.; Utsumi, T.; Moser, D.; Bull, D.; Noréus, D.; Sankey, O.F.; Häussermann, U. Crystal structure, electronic structure, and vibrational properties of  $\text{MAISiH}$  ( $M = \text{Ca, Sr, Ba}$ ): Hydrogenation-induced semiconductors from the  $\text{AlB}_2$ -type alloys  $\text{MAISi}$ . *Phys. Rev. B* **2008**, *78*, 195209. [[CrossRef](#)]
38. Jenkins, H.D.B.; Thakur, K.P. Reappraisal of thermochemical radii for complex ions. *J. Chem. Educ.* **1979**, *56*, 576–577. [[CrossRef](#)]



© 2018 by the authors. Licensee MDPI, Basel, Switzerland. This article is an open access article distributed under the terms and conditions of the Creative Commons Attribution (CC BY) license (<http://creativecommons.org/licenses/by/4.0/>).